THE JOURNAL OF PHYSICAL CHEMISTRY A

Article

pubs.acs.org/JPCA

Supramolecular Dimerization and [2 + 2] Photocycloaddition Reactions of Crown Ether Styryl Dyes Containing a Tethered Ammonium Group: Structure–Property Relationships

Evgeny N. Ushakov,[*,†,‡] Artem I. Vedernikov,[‡] Natalia A. Lobova,[‡] Svetlana N. Dmitrieva,[‡] Lyudmila G. Kuz'mina,[§] Anna A. Moiseeva,[∥] Judith A. K. Howard,[⊥] Michael V. Alfimov,[‡] and Sergey P. Gromov[*,‡,∥]

[†]Institute of Problems of Chemical Physics, Russian Academy of Sciences, Chernogolovka 142432, Moscow Region, Russian Federation

[‡]Photochemistry Center, Russian Academy of Sciences, ul. Novatorov 7A-1, Moscow 119421, Russian Federation

[§]N. S. Kurnakov Institute of General and Inorganic Chemistry, Russian Academy of Sciences, Leninskiy prosp. 31, Moscow 119991, Russian Federation

[∥]Department of Chemistry, M. V. Lomonosov Moscow State University, Leninskie Gory 1, Moscow 119991, Russian Federation

[⊥]Department of Chemistry, Durham University, South Road, Durham DH1 3LE, United Kingdom

Supporting Information

ABSTRACT: Molecular self-assembly is an effective strategy for controlling the [2 + 2] photocycloaddition reaction of olefins. The geometrical properties of supramolecular assemblies are proven to have a critical effect on the efficiency and selectivity of this photoreaction both in the solid state and in solution, but the role of other factors remains poorly understood. Convenient supramolecular systems to study the structure–property relationships are pseudocyclic dimers spontaneously formed by styryl dyes containing a crown ether moiety and a remote ammonium group. New dyes of this type were synthesized to investigate the effects of structural and electronic factors on the quantitative characteristics of supramolecular dimerization and [2 + 2] photocycloaddition in solution. Variable structural parameters for the styryl dyes were the size and structure of macrocyclic moiety, the nature of heteroaromatic residue, and the length of the ammonioalkyl group attached to this residue. Quantum chemical calculations of the pseudocyclic dimers were performed in order to interpret the relationships between the structure of the ammonium dyes and the efficiency of the supramolecular photoreaction. One of the dimeric complexes was obtained in the crystalline state and studied by X-ray diffraction. The results obtained demonstrate that the photocycloaddition in the pseudocyclic dimers can be dramatically affected by the electronic structure of the styryl moieties, as dependent on the electron-donating ability of the substituents on the benzene ring, and by the conformational flexibility of the pseudocycle, which determines the mobility of the olefinic bonds. The significance of electronic factors is highlighted by the fact that the photocycloaddition quantum yield in geometrically similar dimeric structures varies from $\leq 10^{-4}$ to 0.38. The latter value is unusually high for olefins in solution.

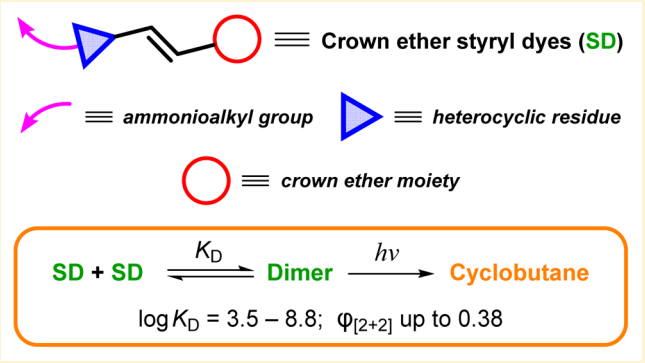

1. INTRODUCTION

The [2 + 2] photocycloaddition (PCA) of olefins is widely used in organic synthesis including the synthesis of pharmaceuticals and natural products.[1,2] Furthermore, it is one of the most useful photoreactions in material chemistry and applied physics.[3]

In homogeneous solutions, diffusion-controlled intermolecular PCA reactions of olefins are normally characterized by very low quantum yields due to short lifetime of the excited state and afford mixtures of cyclobutane isomers. The self-assembly of olefin molecules into pairs with a specific arrangement of the reacting C=C bonds via direct or mediated noncovalent interactions makes it possible not only to activate this photoreaction but also to control its selectivity. To the best of our knowledge, the first example of molecular self-assembly resulting in stereospecific PCA of an acyclic olefin in solution was the formation of 2:2 complexes of a functionalized styrylbenzothiazolium dye with Mg^{2+}.[4] Somewhat earlier, effective photodimerization of tranilast (a cinnamic acid derivative) induced by the 1:2 host–guest complexation with

Received: November 3, 2015
Revised: November 16, 2015

DOI: 10.1021/acs.jpca.5b10758
J. Phys. Chem. A XXXX, XXX, XXX–XXX

γ-cyclodextrin was reported;[5] however, no experimental evidence for the reaction selectivity was provided. The methods of supramolecular chemistry applied to control the PCA of unsaturated compounds in solution are covered most comprehensively in recent reviews.[6,7]

It is well-known that geometrical properties of supramolecular assemblies have a critical effect on the PCA efficiency and selectivity both in the solid phase and in solution;[8] however, the role of other factors remains poorly understood.

The molecules containing a crown ether moiety and a remote ammonium group are able to spontaneously form pseudocyclic dimers in solutions owing to the double macrocycle−ammonium ion interaction involving hydrogen bonds.[9−12] This feature has been used to control the photochemistry of properly modified stilbene[13] and styryl dyes.[14,15] Scheme 1 shows the supramolecular reactions of

Scheme 1. Supramolecular Reactions of 4-Styrylpyridine Derivative 1a[14]

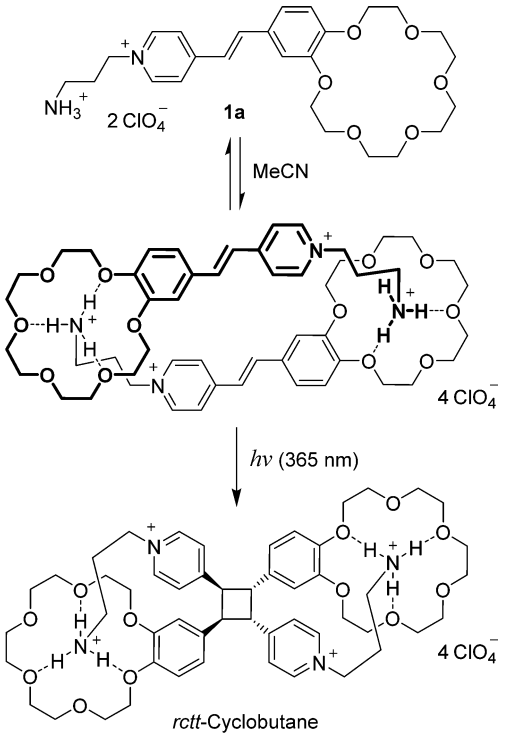

styryl dye **1a** in MeCN. The self-assembly of this dye and its analogues **1b,c** and **2a,b** (Chart 1) into pseudocyclic dimers was found[15] to activate stereospecific PCA, which produces the cyclobutane derivative as the only *rctt* isomer. The degree of conversion of dyes **1a−c** and **2a** to the corresponding *rctt*-cyclobutanes approached 100%.

Here we report the first quantitative study of the structure−property relationships for the supramolecular pseudocyclic dimers of styryl dyes. For a series of dyes containing a tethered ammonium group (compounds **1−6** in Chart1), the dimerization equilibrium constants and the quantum yields of supramolecular PCA were measured in solutions. Quantum chemical modeling of several dimeric complexes was performed in order to interpret the relationships between the structure of the ammonium dyes and the efficiency of the supramolecular photoreaction. An X-ray diffraction study revealed that dye **4a** in the crystalline state exists as a pseudocyclic dimer. The synthesis of ammonium dyes **4a−6a** and model dye **5b** devoid of the ammonium group is reported for the first time.

2. EXPERIMENTAL SECTION

General Methods. ^{1}H and ^{13}C NMR spectra were recorded in DMSO-d_6 using the solvent as the internal reference (δ_H 2.50 and δ_C 39.43). 2D ^{1}H−^{1}H COSY and NOESY spectra and ^{1}H−^{13}C correlation spectra (HSQC and HMBC) were used to assign the proton and carbon signals. The samples for elemental analysis were dried *in vacuo* at 80 °C.

Materials. Acetonitrile (special purity grade, water content <0.03%, v/v), doubly distilled water, 70% perchloric acid (analytical grade), tetrabutylammonium perchlorate (special purity grade) doubly recrystallized from ethanol, and calcium perchlorate (analytical grade) dried *in vacuo* at 230 °C were used in photochemical experiments. Commercial *N*-(4-formylphenyl)aza-18-crown-6 ether, 4′-formylbenzo-18-crown-6 ether, and 3-bromopropylamine hydrobromide were used in the syntheses as received.

Synthesis. Compounds **1−3**,[14,15] **4b**,[16] **6b**,[17] **7a,b**,[15] and **9**[18] were obtained according to published procedures. Dyes **4a**, **5a,b**, and **6a** were synthesized as shown in Scheme 2. The condensation of heterocyclic salts **7a**, **7b**, and **8** with *N*-(4-formylphenyl)aza-18-crown-6 ether in the presence of an organic base afforded dyes **4a**, **5a**, and **5b**, respectively. Compounds **8**, **10a,b** and dye **6a** were synthesized by quaternization of lepidine, 2-methylbenzothiazole, and styrylbenzothiazole **9** with iodoethane and 3-bromopropylamine hydrobromide followed by anion exchange with perchloric acid or $NaClO_4$. Dye **6a** was also obtained by condensation of salt **10b** with 4′-formylbenzo-18-crown-6 ether. The ^{1}H and ^{13}C NMR spectra of **4a**, **5a,b**, **6a**, **8**, and **10a,b** are presented in the Supporting Information (Figures S1−S14). Styryl dyes **4a**, **5a,b**, and **6a** were obtained as the *E* isomers ($^3J_{HC=CH}$ = 15.7−16.2 Hz). All of the synthesized perchlorate salts are nonexplosive substances.

1-(3-Ammoniopropyl)-4-{(*E*)-2-[4-(1,4,7,10,13-pentaoxa-16-azacyclooctadecan-16-yl)phenyl]vinyl}-pyridinium Diperchlorate (4a). A mixture of compound **7a** (130 mg, 0.37 mmol), *N*-(4-formylphenyl)aza-18-crown-6 ether (149 mg, 0.41 mmol), dry pyridine (1 mL), and absolute EtOH (8 mL) was heated at 80 °C (oil bath) for 25 h. After cooling to 5 °C, the precipitate formed was filtered off and washed with cold absolute EtOH (2 × 3 mL) and CH_2Cl_2 (5 mL). The solid was heated at 80 °C with absolute EtOH (5 mL), then cooled to 5 °C, filtered off, and dried in air to give dye **4a** (205 mg, 79% yield) as a red powder: mp 215−217 °C dec; ^{1}H NMR (500.13 MHz, 30 °C) δ 2.15 (m, 2H, $CH_2CH_2NH_3$), 2.84 (br s, 2H, CH_2NH_3), 3.54 (s, 8H, 4 CH_2O), 3.56 (m, 8H, 4 CH_2O), 3.63 (m, 8H, $(CH_2)_2N$, 2 CH_2O), 4.46 (t, ^3J = 7.1 Hz, 2H, CH_2N), 6.81 (d, ^3J = 9.1 Hz, 2H, 3′-H, 5′-H), 7.16 (d, ^3J = 16.2 Hz, 1H, HC=*CH*Py), 7.58 (d, ^3J = 9.1 Hz, 2H, 2′-H, 6′-H), 7.69 (br s, 3H, NH_3), 7.92 (d, ^3J = 16.2 Hz, 1H, *HC*=CHPy), 8.08 (d, ^3J = 6.8 Hz, 2H, 3-H, 5-H), 8.71 (d, ^3J = 6.8 Hz, 2H, 2-H, 6-H) ppm; ^{13}C NMR (125.76 MHz, 30 °C) δ 28.37 ($CH_2CH_2NH_3$), 35.72 (CH_2NH_3), 50.59 ($(CH_2)_2N$), 56.12 (CH_2N), 67.75 ($(CH_2CH_2)_2N$), 69.84 (2 CH_2O), 69.90 (2 CH_2O), 69.97 (4 CH_2O), 111.64 (3′-C, 5′-C), 116.78 (HC=*CH*Py), 122.18 (1′-C), 122.39 (3-C, 5-C), 130.38 (2′-C, 6′-C), 142.28 (HC=CHPy), 143.33 (2-C, 6-C), 149.99 (4′-C), 153.94 (4-C) ppm.

DOI: 10.1021/acs.jpca.5b10758
J. Phys. Chem. A XXXX, XXX, XXX−XXX

Chart 1. Crown Ether Styryl Dyes 1−6

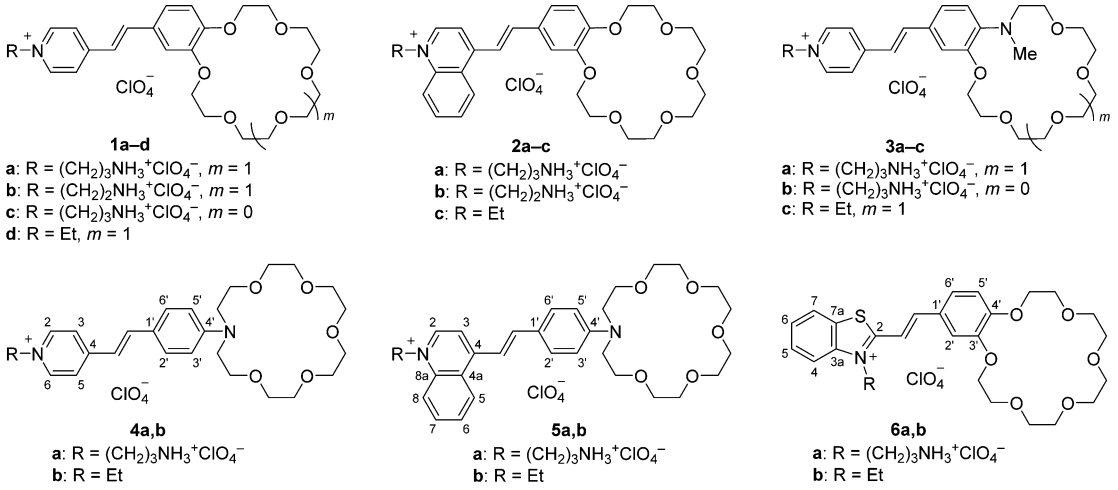

Scheme 2. Synthesis of Dyes 4a, 5a,b, and 6a

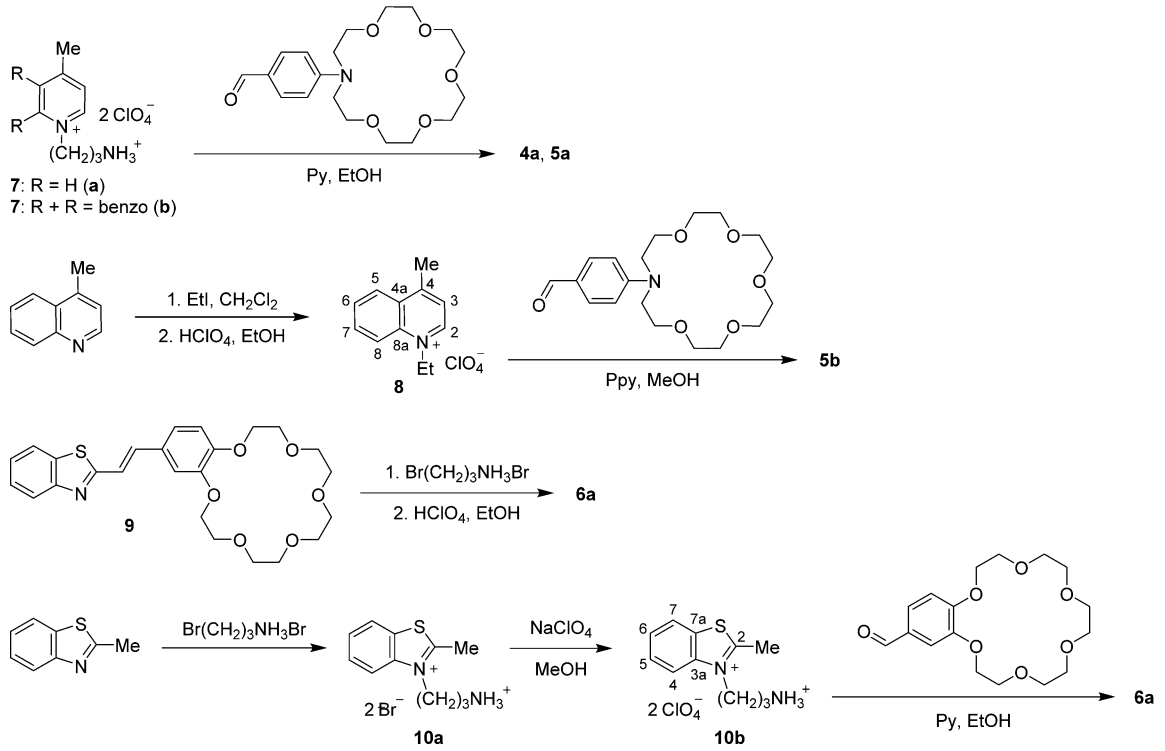

Anal. Calcd for $C_{28}H_{43}Cl_2N_3O_{13}$ (700.56): C, 48.00; H, 6.19; N, 6.00. Found: C, 48.07; H, 6.11; N, 5.97.

1-(3-Ammoniopropyl)-4-{(*E*)-2-[4-(1,4,7,10,13-pentaoxa-16-azacyclooctadecan-16-yl)phenyl]vinyl}-quinolinium Diperchlorate (5a). This was obtained similarly to **4a** from compound **7b** (70 mg, 0.18 mmol) and *N*-(4-formylphenyl)aza-18-crown-6 ether (70 mg, 0.19 mmol) in 85% yield (115 mg) as a dark blue powder: mp 204−206 °C; ^{1}H NMR (500.13 MHz, 30 °C) δ 2.21 (m, 2H, CH_2CH$_2$NH$_3$), 2.96 (m, 2H, CH_2NH$_3$), 3.55 (s, 8H, 4 CH$_2$O), 3.55−3.60 (m, 8H, 4 CH$_2$O), 3.66 (m, 4H, (CH_2CH$_2$)$_2$N), 3.70 (m, 4H, (CH$_2$)$_2$N), 4.91 (t, ^3J = 7.3 Hz, 2H, CH$_2$N), 6.86 (d, ^3J = 9.1 Hz, 2H, 3′-H, 5′-H), 7.70 (br s, 3H, NH$_3$), 7.86 (d, ^3J = 9.1 Hz, 2H, 2′-H, 6′-H), 7.97 (m, 1H, 6-H), 8.02 (d, ^3J = 15.7 Hz, 1H, HC═C*H*Het), 8.19 (d, ^3J = 15.7 Hz, 1H, *H*C═CHHet), 8.21 (m, 1H, 7-H), 8.36 (d, ^3J = 6.8 Hz, 1H, 3-H), 8.43 (d, ^3J = 9.1 Hz, 1H, 8-H), 9.05 (d, ^3J = 9.1 Hz, 1H, 5-H), 9.07 (d, ^3J = 6.8 Hz, 1H, 2-H) ppm; ^{13}C NMR (125.76 MHz, 30 °C) δ 27.05 (CH$_2$CH$_2$NH$_3$), 36.11 (CH$_2$NH$_3$), 50.69 ((CH$_2$)$_2$N), 52.91 (CH$_2$N), 67.82 ((CH$_2$CH$_2$)$_2$N), 69.85 (2 CH$_2$O), 69.92 (2 CH$_2$O), 70.00 (4 CH$_2$O), 111.74 (3′-C, 5′-C), 112.90 (HC═*C*HHet), 114.03 (3-C), 118.51 (8-C), 122.91 (1′-C), 126.11 (4a-C), 126.66 (5-C), 128.40 (6-C), 131.61 (2′-C, 6′-C), 134.70 (7-C), 137.81 (8a-C), 145.10 (HC═CHHet), 145.92 (2-C), 150.60 (4′-C), 153.58 (4-C) ppm; UV−vis (MeCN) λ_{max} (ε) = 239 (19900), 309 (12300), 558 nm (37100 M^{-1}·cm^{-1}). Anal. Calcd for $C_{32}H_{45}Cl_2N_3O_{13}$ (750.62): C, 51.20; H, 6.04; N, 5.60. Found: C, 51.28; H, 6.01; N, 5.61.

1-Ethyl-4-methylquinolinium Perchlorate (8). A solution of lepidine (2.00 mL, 15.15 mmol) and EtI (1.83 mL, 22.72 mmol) in CH_2Cl_2 (15 mL) was kept at room temperature in the dark for 17 days. The solvent was

DOI: 10.1021/acs.jpca.5b10758
J. Phys. Chem. A XXXX, XXX, XXX−XXX

evaporated *in vacuo*, and the residue was triturated with benzene (15 mL). The insoluble fraction was filtered off, washed with benzene (3 × 15 mL), and dried *in vacuo* at 80 °C to give 1-ethyl-4-methylquinolinium iodide (3.67 g, 81% yield) as a yellow-green powder: mp 142−143 °C (lit.:[19] mp 143−144 °C); ^{13}C NMR (125.76 MHz, 25 °C) δ 15.10 (*Me*CH_2), 19.60 (*Me*Het), 52.39 (CH_2N), 119.10 (8-C), 122.66 (3-C), 127.05 (5-C), 128.77 (4a-C), 129.43 (6-C), 134.97 (7-C), 136.41 (8a-C), 147.96 (2-C), 158.23 (4-C) ppm. The iodide salt (1.08 g, 3.61 mmol) was dissolved at heating in a minimum quantity of absolute EtOH. After the addition of 70% $HClO_4$(aq) (0.29 mL, 3.34 mmol) and cooling to −10 °C, the precipitate formed was filtered off, washed with cold absolute EtOH (2 × 3 mL), and dried in air to give compound **8** (0.38 g, 39% yield) as a light yellow crystalline powder: mp 128−130 °C; ^{1}H NMR (500.13 MHz, 30 °C) δ 1.59 (t, ^3J = 7.3 Hz, 3H, *Me*CH_2), 3.00 (s, 3H, *Me*Het), 5.04 (q, ^3J = 7.3 Hz, 2H, CH_2N), 8.05 (m, 1H, 6-H), 8.06 (d, ^3J = 6.6 Hz, 1H, 3-H), 8.26 (m, 1H, 7-H), 8.55 (d, ^3J = 8.6 Hz, 1H, 5-H), 8.59 (d, ^3J = 9.1 Hz, 1H, 8-H), 9.39 (d, ^3J = 6.6 Hz, 1H, 2-H) ppm; ^{13}C NMR (125.76 MHz, 26 °C) δ 15.09 (*Me*CH_2), 19.54 (*Me*Het), 52.43 (CH_2N), 119.10 (8-C), 122.72 (3-C), 127.09 (5-C), 128.85 (4a-C), 129.48 (6-C), 135.03 (7-C), 136.50 (8a-C), 148.01 (2-C), 158.35 (4-C) ppm. Anal. Calcd for $C_{12}H_{14}ClNO_4$ (271.70): C, 53.05; H, 5.19; N, 5.16. Found: C, 53.08; H, 5.14; N, 5.09.

1-Ethyl-4-{(*E*)-2-[4-(1,4,7,10,13-pentaoxa-16-azacyclooctadecan-16-yl)phenyl]vinyl}quinolinium Perchlorate (5b). A mixture of compound **8** (200 mg, 0.74 mmol), *N*-(4-formylphenyl)aza-18-crown-6 ether (300 mg, 0.81 mmol), dry piperidine (40 μL), and MeOH (10 mL) was heated at 70 °C (oil bath) for 27 h. The solvent was evaporated *in vacuo*, and the residue was washed with hot benzene (4 × 20 mL) and absolute EtOH (2 × 10 mL). The insoluble fraction was decanted and dried in air to give dye **5b** (430 mg, 94% yield) as a dark violet glassy solid: mp 86−88 °C; ^{1}H NMR (500.13 MHz, 30 °C) δ 1.56 (t, ^3J = 7.1 Hz, 3H, Me), 3.54 (s, 8H, 4 CH_2O), 3.55−3.58 (m, 8H, 4 CH_2O), 3.64 (m, 4H, (CH_2CH_2)$_2$N), 3.67 (m, 4H, (CH_2)$_2$N), 4.90 (q, ^3J = 7.1 Hz, 2H, CH_2N), 6.83 (d, ^3J = 8.9 Hz, 2H, 3′-H, 5′-H), 7.82 (d, ^3J = 8.9 Hz, 2H, 2′-H, 6′-H), 7.94 (m, 1H, 6-H), 7.96 (d, ^3J = 15.7 Hz, 1H, HC═C*H*Het), 8.13 (d, ^3J = 15.7 Hz, 1H, *H*C═CHHet), 8.17 (m, 1H, 7-H), 8.31 (d, ^3J = 6.7 Hz, 1H, 3-H), 8.40 (d, ^3J = 8.7 Hz, 1H, 8-H), 8.98 (d, ^3J = 8.7 Hz, 1H, 5-H), 9.11 (d, ^3J = 6.7 Hz, 1H, 2-H) ppm; ^{13}C NMR (125.76 MHz, 30 °C) δ 14.87 (Me), 50.65 ((CH_2)$_2$N), 51.26 (CH_2N), 67.80 ((CH_2CH_2)$_2$N), 69.83 (2 CH_2O), 69.91 (2 CH_2O), 69.98 (4 CH_2O), 111.63 (3′-C, 5′-C), 112.94 (HC═CHHet), 114.11 (3-C), 118.51 (8-C), 122.88 (1′-C), 125.97 (4a-C), 126.49 (5-C), 128.30 (6-C), 131.41 (2′-C, 6′-C), 134.61 (7-C), 137.52 (8a-C), 144.57 (HC═CHHet), 145.63 (2-C), 150.40 (4′-C), 153.12 (4-C) ppm; UV−vis (MeCN) λ_{max} (ε) = 236 (23500), 307 (13100), 542 nm (28700 $M^{-1}\cdot cm^{-1}$). Anal. Calcd for $C_{31}H_{41}ClN_2O_9$ (621.12): C, 59.95; H, 6.65; N, 4.51. Found: C, 59.87; H, 6.51; N, 4.58.

3-(3-Ammoniopropyl)-2-methyl-1,3-benzothiazol-3-ium Dibromide (10a). A mixture of 2-methylbenzothiazole (1.34 mL, 10.58 mmol) and 3-bromopropylamine hydrobromide (1.55 g, 7.06 mmol) was heated at 150 °C (oil bath) for 24 h. After cooling to room temperature, the reaction mixture was triturated with benzene (3 × 10 mL), MeCN (3 × 10 mL), and *i*-PrOH (3 × 10 mL). The insoluble substance was filtered off, washed with *i*-PrOH (2 × 10 mL), and dried in air to give compound **10a** (1.95 g, 75% yield) as a light-gray powder: mp 278−279 °C dec; ^{1}H NMR (500.13 MHz, 24 °C) δ 2.16 (m, 2H, C$H_2CH_2NH_3$), 3.07 (m, 2H, CH_2NH_3), 3.21 (s, 3H, Me), 4.81 (m, 2H, CH_2N), 7.82 (m, 1H, 6-H), 7.90 (br s, 3H, NH_3), 7.92 (m, 1H, 5-H), 8.40 (d, ^3J = 8.5 Hz, 1H, 4-H), 8.48 (d, ^3J = 8.0 Hz, 1H, 7-H) ppm; ^{13}C NMR (125.76 MHz, 25 °C) δ 17.15 (Me), 25.59 ($CH_2CH_2NH_3$), 35.90 (CH_2NH_3), 46.51 (CH_2N), 116.68 (4-C), 124.69 (7-C), 127.96 (6-C), 129.12 (7a-C), 129.22 (5-C), 140.70 (3a-C), 177.71 (2-C) ppm. Anal. Calcd for $C_{11}H_{16}Br_2N_2S$ (368.13): C, 35.89; H, 4.38; N, 7.61. Found: C, 35.64; H, 4.31; N, 7.51.

3-(3-Ammoniopropyl)-2-methyl-1,3-benzothiazol-3-ium Diperchlorate (10b). Compound **10a** (507 mg, 1.38 mmol) was dissolved at heating in a mixture of MeOH (12 mL) and water (0.3 mL). A solution of $NaClO_4$ (408 mg, 3.32 mmol) in MeOH (1 mL) was added to the solution of compound **10a**, and the reaction mixture was cooled to −10 °C. The precipitate formed was filtered off, washed with cold absolute EtOH (2 × 5 mL), and dried in air to give compound **10b** (510 mg, 91% yield) as light-beige crystals: mp 257−258 °C dec; ^{1}H NMR (500.13 MHz, 26 °C) δ 2.12 (m, 2H, C$H_2CH_2NH_3$), 3.04 (m, 2H, CH_2NH_3), 3.18 (s, 3H, Me), 4.76 (m, 2H, CH_2N), 7.76 (br s, 3H, NH_3), 7.83 (m, 1H, 6-H), 7.93 (m, 1H, 5-H), 8.34 (d, ^3J = 8.6 Hz, 1H, 4-H), 8.46 (d, ^3J = 8.2 Hz, 1H, 7-H) ppm; ^{13}C NMR (125.76 MHz, 25 °C) δ 16.82 (Me), 25.65 ($CH_2CH_2NH_3$), 36.01 (CH_2NH_3), 46.34 (CH_2N), 116.49 (4-C), 124.66 (7-C), 128.08 (6-C), 129.17 (7a-C), 129.29 (5-C), 140.71 (3a-C), 177.79 (2-C) ppm. Anal. Calcd for $C_{11}H_{16}Cl_2N_2O_8S$ (407.22): C, 32.44; H, 3.96; N, 6.88. Found: C, 32.51; H, 4.07; N, 6.81.

3-(3-Ammoniopropyl)-2-[(*E*)-2-(2,3,5,6,8,9,11,12,-14,15-decahydro-1,4,7,10,13,16-benzohexaoxacyclooctadecin-18-yl)vinyl]-1,3-benzothiazol-3-ium Diperchlorate (6a). *Method A.* A mixture of compound **9** (150 mg, 0.32 mmol) and 3-bromopropylamine hydrobromide (209 mg, 0.96 mmol) was heated at 150 °C (oil bath) in the dark for 4 h. The reaction mixture was extracted with hot absolute EtOH (3 × 5 mL, cooling to −10 °C before decantation). The insoluble fraction (171 mg) was dissolved at heating in a mixture of EtOH (10 mL) and water (several drops). After the addition of 70% $HClO_4$(aq) (95 μL, 1.18 mmol) and cooling to −10 °C, the precipitate formed was decanted and recrystallized from aqueous EtOH (5 mL) containing 70% $HClO_4$ (aq) (45 μL, 0.56 mmol). The solid was filtered off, washed with absolute EtOH (5 mL), and dried in air to give dye **6a** (53 mg, 22% overall yield) as an orange powder: mp 250−252 °C; ^{1}H NMR (500.13 MHz, 25 °C) δ 2.14 (m, 2H, C$H_2CH_2NH_3$), 3.00 (m, 2H, CH_2NH_3), 3.54 (s, 4H, 2 CH_2O), 3.57 (m, 4H, 2 CH_2O), 3.64 (m, 4H, 2 CH_2O), 3.80 (m, 2H, CH_2CH_2OAr), 3.83 (m, 2H, CH_2CH_2OAr), 4.23 (m, 4H, 2 CH_2OAr), 4.98 (t, ^3J = 7.3 Hz, 2H, CH_2N), 7.18 (d, ^3J = 8.6 Hz, 1H, 5′-H), 7.65 (br s, 1H, 2′-H), 7.69 (br d, ^3J = 8.6 Hz, 1H, 6′-H), 7.71 (br s, 3H, NH_3), 7.78 (d, ^3J = 15.7 Hz, 1H, HC═C*H*Het), 7.80 (m, 1H, 6-H), 7.90 (m, 1H, 5-H), 8.23 (d, ^3J = 15.7 Hz, 1H, *H*C═CHHet), 8.28 (d, ^3J = 8.6 Hz, 1H, 4-H), 8.45 (d, ^3J = 8.2 Hz, 1H, 7-H) ppm; ^{13}C NMR (125.76 MHz, 30 °C) δ 26.46 ($CH_2CH_2NH_3$), 36.03 (CH_2NH_3), 45.71 (CH_2N), 68.34 (CH_2OAr), 68.51 (CH_2OAr), 69.57 (CH_2O), 69.68 (5 CH_2O), 69.79 (CH_2O), 69.84 (CH_2O), 110.35 (HC═*C*HHet), 112.71 (5′-C), 113.31 (2′-C), 116.14 (4-C), 124.30 (7-C), 125.63 (6′-C), 126.70 (1′-C), 127.90 (7a-C), 128.14 (6-C), 129.27 (5-C), 141.10 (3a-C), 148.35 (3′-C), 149.83 (HC═CHHet), 152.64 (4′-C), 172.36 (2-C) ppm. Anal. Calcd for $C_{28}H_{38}Cl_2N_2O_{14}S\cdot 0.5H_2O$

DOI: 10.1021/acs.jpca.5b10758
J. Phys. Chem. A XXXX, XXX, XXX−XXX

(738.59): C, 45.53; H, 5.32; N, 3.79. Found: C, 45.56; H, 5.17; N, 3.30.

Method B. A mixture of compound **10b** (80 mg, 0.20 mmol), 4′-formylbenzo-18-crown-6 ether (74 mg, 0.22 mmol), dry pyridine (0.5 mL), and absolute EtOH (10 mL) was heated at 85 °C (oil bath) for 34 h. After cooling to room temperature, a yellowish orange precipitate (43 mg) was filtered off and then triturated with absolute EtOH (2 × 2 mL) at heating. The insoluble substance was filtered off, washed with absolute EtOH (2 × 0.5 mL) and dried in air to give dye **6a** (31 mg, 21% yield) as a yellowish orange powder: mp 252−253 °C.

Dimerization Equilibrium Constants. The supramolecular dimerization of ammonium dyes **1**−**4** and **6** was studied by spectrophotometry in MeCN and MeCN−H_2O (94:6, v/v) solutions at an ionic strength of 0.01 M (Bu_4NClO_4 as the supporting electrolyte). The solutions contained minor amounts of $HClO_4$ (1×10^{-5} M), which ruled out the possible deprotonation of the ammonium group of the dye by nucleophilic impurities in MeCN (in experiments involving azacrown dyes, the acid was not used). The absorption spectra of solutions with different total dye concentrations ($C_L = 2 \times 10^{-6}$ to 2×10^{-3} M) were measured in quartz cells with an optical path length of 50, 10, 2, 1, 0.5, and 0.1 mm. The resulting spectra were subjected to parametrized matrix modeling[20,21] in terms of the dimerization equilibrium:

$$L^{2+} + L^{2+} \overset{K_D}{\rightleftarrows} L_2^{4+} \quad (1)$$

where L^{2+} is the dye dication, L_2^{4+} is the dimeric complex, and K_D (M^{-1}) is the dimerization equilibrium constant. This method is suitable for simultaneous calculation of K_D and the absorption spectra of the monomer and dimer.

The exact C_L value after dilution of a 2×10^{-3} M stock solution was determined from the optical density at the wavelength where the monomer and the dimer have equal molar absorption coefficients (per monomer). The isosbestic point was found beforehand from the absorption spectra measured in the absence of a supporting electrolyte and after addition of a weighed portion of Bu_4NClO_4 (an increase in the solution ionic strength shifted the monomer−dimer equilibrium toward the dimer, see Figure S15 in the Supporting Information).

^{1}H NMR Titration. MeCN-d_3 (water content <0.05%, v/v) was used as the solvent. The dimerization constants K_D for ammonium dyes **4a**−**6a** were estimated by analyzing the changes in the chemical shifts of the aromatic and ethylene protons of dye, $\Delta\delta_H$, induced by an incremental addition of $EtNH_3ClO_4$, as described previously for ammonium dyes **1**−**3**.[15] In these experiments, the C_L value was kept constant (~1×10^{-3} or ~5×10^{-3} M) and the total concentration of $EtNH_3ClO_4$ (C_S) varied from 0 to ~$50C_L$. The $\Delta\delta_H$ values were measured to an accuracy of 0.001 ppm. The experimental dependencies of $\Delta\delta_H$ on C_S for different protons were globally fitted to the complexation model represented by eqs 1 and 2:

$$L^{2+} + EtNH_3^+ \overset{K_1}{\rightleftarrows} (L{\cdot}EtNH_3)^{3+} \quad (2)$$

These calculations were performed under the assumption that the complex stability constant K_1 (M^{-1}) for the dicationic dye is equal to that for the corresponding model dye having no ammonium group. The K_1 values for model dyes **4b**−**6b** were estimated from direct ^{1}H NMR titrations with $EtNH_3ClO_4$ and then used as fixed parameters in the calculations of K_D for **4a**−**6a**. The equilibrium constants were calculated using the HYPNMR program.[22]

X-ray Diffraction Crystal Structure Determination and Crystal Data. The crystals of dye **4a** were grown from a MeCN solution, which was slowly saturated with benzene by vapor diffusion method at ambient temperature. The single crystal was coated with perfluorinated oil and mounted on a CCD diffractometer [graphite monochromatized Cu Kα radiation (λ = 1.54178 Å), ω scan mode] under a stream of cold nitrogen. A set of experimental reflections was measured, and the structure was solved by direct methods and refined with anisotropic thermal parameters for all non-hydrogen atoms. Absorption correction was applied using the SADABS method. The hydrogen atoms were fixed at calculated positions at C and N atoms and then refined using the "riding" model.

*Data for **4a**.* $C_{28}H_{43}Cl_2N_3O_{13}$, M = 700.55, monoclinic, space group $P2_1$ (No. 4), red block, a = 9.8760(3), b = 21.0048(6), c = 15.9354(5) Å, β = 92.053(2)°, V = 3303.57(17) Å^3, T = 120(2) K, Z = 4, μ = 2.361 mm^{-1}, ρ_{calcd} = 1.409 g cm^{-3}, $2\theta_{max}$ = 151.4°, 38916 reflections measured, 12594 unique (R_{int} = 0.0635), R_1 = 0.0548 (10050 reflections with $I > 2\sigma(I)$), wR_2 = 0.1453 (all data), goodness-of-fit on F^2 = 1.015, 932 parameters, min/max residual electron density = −0.35/0.73 e Å^{-3}. One of the four independent perchlorate anions in structure **4a** is disordered over two positions with an occupancy ratio of 0.90:0.10, and the Het−C═C−Ar moiety of one of the two independent organic cations is disordered over two positions with an occupancy ratio of 0.83:0.17. ISOR command was applied to the atoms of the disordered groups in order to constrain their anisotropic thermal parameters.

The calculations were performed using the SHELXTL-Plus[23] and Olex-2[24] software. CCDC 1426657 contains the supplementary crystallographic data for **4a**. These data can be obtained free of charge from the Cambridge Crystallographic Data Center via www.ccdc.cam.ac.uk/data_request/cif.

Density Functional Theory (DFT) Calculations. All DFT calculations were performed using the Gaussian 09 program package.[25] Geometry optimizations were carried out using the B3LYP functional,[26] the D3(BJ) dispersion correction,[27] the 6-31G(d) basis set, and the C-PCM solvation model.[28] The fractional conformer populations in MeCN at 295 K were estimated using the Boltzmann distribution function under the assumption that thermal corrections to the B3LYP-D3/PCM energies of different conformers are identical.

Quantum Yields of Supramolecular [2 + 2] Photocycloaddition. Photochemical studies of ammonium dyes **1**−**6** were conducted in MeCN solutions at an ionic strength of 0.01 M. Solutions were exposed to glass-filtered light of a high-pressure Hg lamp (λ = 436 nm). The light intensity was measured by chemical actinometry. The concentration of dyes before irradiation was about 3×10^{-5} M (10 mm cell, dyes with log K_D > 7) or about 1.5×10^{-4} M (2 mm cell, dyes with log K_D < 7). The percentage of consumption of the dye in the supramolecular PCA reaction was determined using unconventional photochemical method described in the Supporting Information (Figures S16−S18).

For monomer−dimer systems that underwent no photoreactions other than PCA and in which the relative monomer content in the equilibrium mixture was negligibly low, the quantum yield of supramolecular PCA reaction, $\varphi_{[2+2]}$, was determined from the kinetics of the absorption spectra observed in the initial stage of dye photolysis. The time-dependent spectra were subjected to parametrized matrix

DOI: 10.1021/acs.jpca.5b10758
J. Phys. Chem. A XXXX, XXX, XXX−XXX

modeling in terms of the kinetic equation for irreversible unimolecular photoreactions

$$\frac{dC_L(t)}{dt} = \varphi_{[2+2]} I N_A^{-1} 10^3 \frac{(1 - 10^{-\varepsilon C_L(t) l})}{l} \quad (3)$$

where I is the light intensity, cm^{-2} s^{-1}; N_A is the Avogadro number, mol^{-1}; ε is the molar absorption coefficient of the dimer at 436 nm (per monomer), M^{-1} cm^{-1}; and l is the cell length, cm.

For the monomer−dimer systems in which the relative monomer content in the equilibrium mixture was rather high, the $\varphi_{[2+2]}$ value was estimated from the formula

$$\varphi_{[2+2]} = \frac{\Delta C_L}{t_{ir} I N_A^{-1} 10^3 l A}, \quad A = \frac{1}{2}\left\{\frac{D_0'}{D_0}(1 - 10^{-D_0}) + \frac{D_{ir}'}{D_{ir}}(1 - 10^{-D_{ir}})\right\} \quad (4)$$

where ΔC_L is the overall consumption of the dye in the PCA reaction during the irradiation time t_{ir}; D_0 and D_{ir} are the total optical densities of solution at 436 nm before and after irradiation; D_0' and D_{ir}' are the contributions from the dimer to the total optical densities at 436 nm before and after irradiation. The $(D_0 - D_{ir})/D_0$ value did not exceed 0.2.

3. RESULTS AND DISCUSSION

3.1. Supramolecular Dimerization. *3.1.1. Spectrophotometric Data.* Figure 1 shows the absorption spectra of dye **1a** at different concentrations in MeCN−H_2O solution (94:6, v/v) at an ionic strength of 0.01 M.

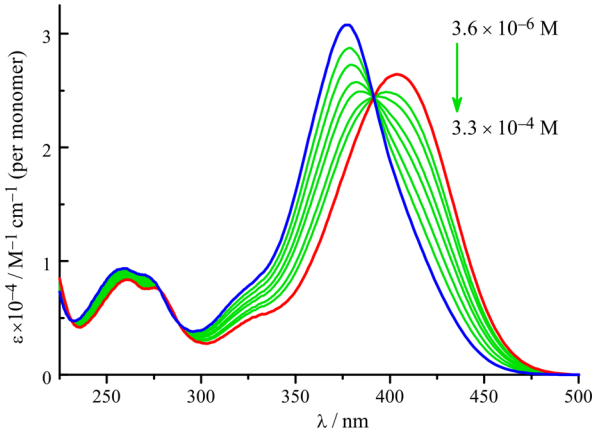

Figure 1. Green curves are the absorption spectra of dye **1a** at different concentrations in MeCN−H_2O solution (94:6, v/v); the ionic strength of the solution was maintained at 0.01 M (supporting electrolyte Bu_4NClO_4). The red and blue curves are the spectra of monomer **1a** and dimer $(\mathbf{1a})_2$, respectively, as derived from global fitting of the concentration-dependent spectra to the equilibrium of eq 1.

Styryl dyes **1**−**6** have a structure typical of donor−acceptor chromoionophores demonstrating hypsochromic shifts upon complexation with metal or ammonium cations.[29,30] The fact that an increase in the concentration of **1a** induces a substantial hypsochromic effect attests to self-complexation of the dye, namely, to the formation of pseudocyclic dimers due to the double macrocycle−ammonium ion interaction (see Scheme 1). Similar spectral properties are exhibited by other ammonium dyes shown in Chart 1 (see Figures S19−S27 in the Supporting Information). The long-wavelength absorption band of the dimer $(\mathbf{1a})_2$ has an asymmetric shape typical of dye *H*-aggregates,[31] which attests to stacking interactions between the chromophores. A good example of the effect of these interactions on the spectral properties of unsaturated compounds is provided by the stacked dimers of a functionalized butadienyl dye.[32] The absorption band of dimer $(\mathbf{1b})_2$ (Figure S19) has a more clear-cut asymmetry than that of $(\mathbf{1a})_2$. This is caused by the fact that the relatively short ammonioethyl spacers in dimer $(\mathbf{1b})_2$ ensure stronger stacking interactions between the chromophores.

The dimerization equilibrium constant K_D and the absorption spectra of the monomer and dimer were calculated by global fitting of concentration-dependent spectra of the dye to the equilibrium of eq 1 (see the Experimental Section). The log K_D values and the main spectrophotometric characteristics of ammonium dyes **1**−**4** and **6** in MeCN and MeCN−H_2O solutions at an ionic strength of 0.01 M are presented in Table 1.

The log K_D values in MeCN for some dyes that are highly prone to dimerization were estimated with the assumption that $\Delta\log K_D = \log K_D(\text{MeCN}) - \log K_D(\text{MeCN–H}_2\text{O})$ is determined by the difference between the free energies of solvation of the ammonium group in the two solvents and almost independent of the chromophore structure.[33] This assumption relies on the fact that the dimerization is driven by the macrocycle−ammonium ion interactions. The approximate log K_D values were calculated using $\Delta\log K_D = 2.7$ measured for dye **6a**.

It is noteworthy that the absorption spectra of the pseudocyclic dimers of ammonium dyes in MeCN are almost identical to those in MeCN−H_2O solution (see data for **1**−**3** and **6** in Table 1 and Figures 19−27 in the Supporting Information). This fact suggests that in the mixed solvent, there are no specific interactions of water molecules with the stacked styryl moieties of the pseudocyclic dimers.

Recent investigations have demonstrated that styryl dyes containing an *N*-methylbenzoazacrown ether moiety such as model dye **3c** exhibit stronger ionochromic responses to metal cations in comparison with benzocrown- and *N*-phenylazacrown-containing analogues.[34] Therefore, it is not surprising that compounds **3a,b**, among the other ammonium dyes tested, exhibit the largest hypsochromic shifts upon dimerization.

In MeCN, the dimerization equilibrium constants vary over a very wide range (more than 5 orders of magnitude) depending on the structure of the ammonium dye. The observed correlations are discussed in section 3.1.5.

3.1.2. ^{1}H NMR Spectroscopic Data. Recently, it was shown by NMR spectroscopy that ammonium dyes **1a**−**c**, **2a**, and **3a,b** are able to form pseudocyclic head-to-tail dimers in MeCN-d_3.[15]

Figure 2 shows the ^{1}H NMR spectra of new ammonium dye **4a**, its analogue **4b** having no ammonium group, and a mixture of **4b** with $EtNH_3ClO_4$ (the proton numbering is shown in Chart 1). The signals of ethylene and most aromatic protons of dye **4a** capable of self-complexation are shifted upfield ($\Delta\delta_H$ of up to −0.25 ppm) with respect to the signals of model dye **4b** (Figure 2*a*,*c*). All proton signals of **4b** shift downfield upon coordination of $EtNH_3^+$ to the crown ether moiety of the dye (Figure 2*a*,*b*). These facts indicate strong anisotropic effects of the chromophore moieties[15] in the pseudocyclic dimer $(\mathbf{4a})_2$.

DOI: 10.1021/acs.jpca.5b10758
J. Phys. Chem. A XXXX, XXX, XXX−XXX

Table 1. Dimerization Equilibrium Constants (K_D) and Spectrophotometric Characteristics of Ammonium Dyes 1−4 and 6 in MeCN and MeCN−H_2O Solutions at an Ionic Strength of 0.01 M[a]

	MeCN				MeCN−H_2O (96:4, v/v)			
dye	log K_D	λ_{max} dimer/dye	$\Delta\lambda$	$\varepsilon_{max} \times 10^{-4}$ dimer/dye	log K_D	λ_{max} dimer/dye	$\Delta\lambda$	$\varepsilon_{max} \times 10^{-4}$ dimer/dye
1a	7.3[b]	378			4.6	378/404	26	3.07/2.64
1b	8.1[b]	383			5.4	383/409	26	3.17/2.96
1c	3.5	379/404	25	2.94/2.85	<1.3			
2a	7.7[b]	419			5.0	419/450	31	2.70/2.17
2b	7.4[b]	429			4.7	428/453	25	2.57/2.30
3a	8.8[b]	391			6.1	390/465	75	2.27/2.54
3b	3.7	391/468	77	2.36/2.64	<1.3			
4a	3.6	415/487	72	3.27/4.42	<1.3			
6a	6.1	418/433	15	3.50/3.64	3.4	417/432	15	3.49/3.60

[a]Supporting electrolyte, Bu_4NClO_4; ambient temperature; λ_{max} is the long-wavelength absorption maximum, nm; $\Delta\lambda = \lambda_{max}$(dye) − λ_{max}(dimer); ε_{max} is the molar absorption coefficient at λ_{max} (per monomer), M^{-1} cm^{-1}; the K_D values are measured to within 10−20%. [b]Estimated using a difference of 2.7 between the log K_D(MeCN) and log K_D(MeCN−H_2O) values measured for dye **6a**.

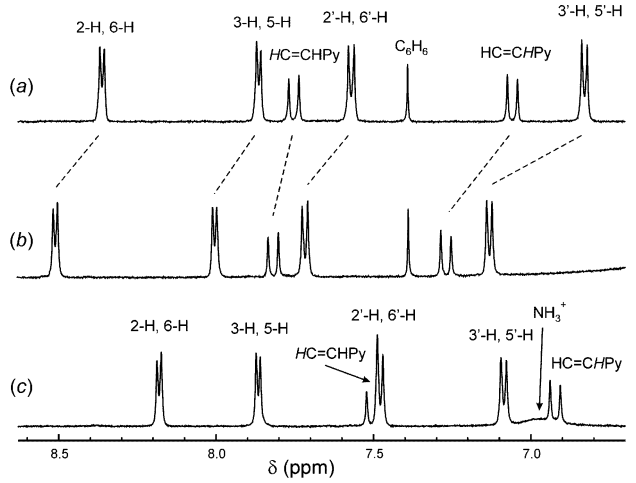

Figure 2. ^{1}H NMR spectra (aromatic proton region) of (*a*) dye **4b**, (*b*) a 1:22 mixture of **4b** with $EtNH_3ClO_4$, and (*c*) dye **4a** at a concentration of 5×10^{-3} M (500.13 MHz, MeCN-d_3, 25 °C).

Dyes **5a,b** and **6a,b** show similar spectral properties (see Figures S28 and S29 in the Supporting Information).

Table 2 presents the dimerization equilibrium constants for ammonium dyes **4a−6a** and the stability constants for the 1:1 complexes of model dyes **4b−6b** with $EtNH_3^+$, as derived from ^{1}H NMR titrations with $EtNH_3ClO_4$ (see the Experimental Section). The Table is supplemented by published data for ammonium dyes **1a−3a** and the corresponding model compounds.

Table 2. Dimerization Equilibrium Constants (K_D) for Ammonium Dyes and Stability Constants (K_1) for the 1:1 Complexes of Related Model Dyes with $EtNH_3^+$, as Derived from ^{1}H NMR Titrations with $EtNH_3ClO_4$[a]

dye	log K_D	dye	log K_1
3a	8.2[b]	**3c**	3.9[b]
2a	8.0[b]	**1d**	3.6[b]
1a	7.1[b]	**2c**	3.5[b]
6a	5.9	**6b**	3.5[c]
5a	3.9	**4b**	1.9
4a	3.6	**5b**	1.7

[a]MeCN-d_3, 25 ± 1 °C; the equilibrium constants are measured to within about 30%. [b]Reference 15. [c]Reference 17.

The log K_D values estimated by ^{1}H NMR titration are consistent at a qualitative level with the data obtained by spectrophotometry (see Table 1). What is most important is that the dependences of log K_D on the dye structure are similar for the two methods. Some discrepancies in the absolute magnitudes of log K_D are attributable to the fact that in both cases, the dimerization constants were calculated with certain assumptions and that the solution ionic strength was not fixed in the ^{1}H NMR titration experiments.

The constants K_D for dyes **4a** and **5a** do not exceed 10^4 M^{-1} and, therefore, they can be estimated by measuring the concentration dependence of the ^{1}H NMR spectrum. Figures S30 and S31 (see the Supporting Information) show the changes in the proton chemical shifts of these dyes, $\Delta\delta_H$, as induced by incremental increase in the dye concentration. In both cases, as the dye concentration increases, the signals of aromatic and ethylene protons and methylene protons of the ammoniopropyl group shift mainly upfield ($\Delta\delta_H$ of up to −0.51 ppm), while the proton signals from most crown ether CH_2O groups shift downfield. The dependencies of $\Delta\delta_H$ on C_L were fitted to a monomer−dimer equilibrium model to give log K_D = 3.7 for **4a** and 3.2 for **5a**. In the case of **4a**, the calculated log K_D value is in good agreement with that estimated from the data of titration with $EtNH_3ClO_4$. However, in the case of **5a**, the log K_D values obtained by the two methods are considerably different (3.2 vs 3.9). Apparently, dye **5a** having more extended conjugated system than **4a** is more prone to form stacked supramolecular assemblies with an aggregation number of >2. Even a small presence of these assemblies at high dye concentrations can introduce a substantial error into the calculation of K_D.

3.1.3. X-ray Diffraction Analysis. Previously, it was shown[15] that dyes **1b** and **2b** exist in the crystalline state as pseudocyclic dimers and that dye **1b** undergoes solid-phase PCA, which induces single crystal-to-single crystal transformation.

Single crystals suitable for X-ray diffraction were also obtained for the new dye **4a**. The independent unit cell components are shown in Figure 3. This is the first crystal structure of a complex between an *N*-phenylaza-18-crown-6 ether and an ammonium ion.

The two organic dications in structure **4a** form a head-to-tail pseudocyclic dimer due to double macrocycle−ammonium ion interaction. The azacrown ether moieties of the dications have

DOI: 10.1021/acs.jpca.5b10758
J. Phys. Chem. A XXXX, XXX, XXX−XXX

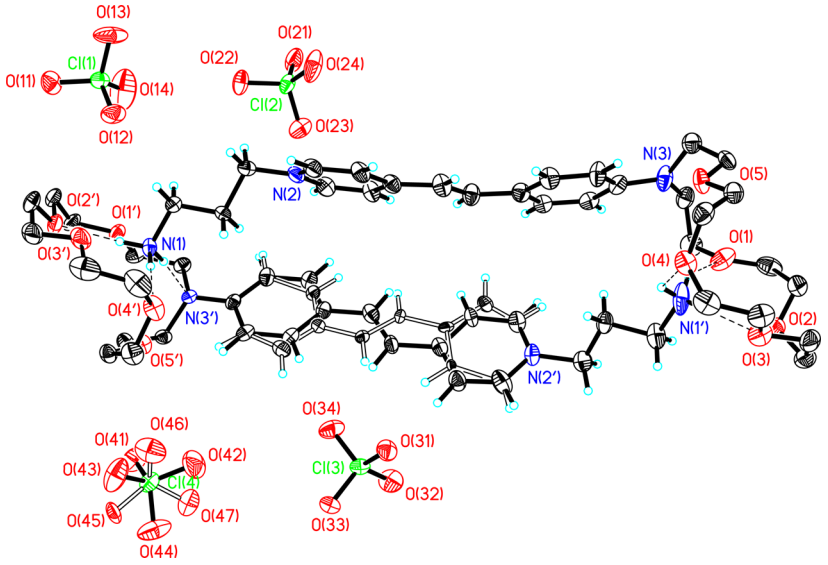

Figure 3. Structure **4a** (two independent dye molecules forming dimeric complex). Thermal ellipsoids are drawn at the 40% probability level. The hydrogen atoms of crown ether moieties are omitted for clarity. Hydrogen bonds are drawn with dashed lines. Minor conformers of the disordered parts are drawn with hollow lines.

extended and fairly twisted conformations. Poor preorganization of *N*-phenylazacrown ethers toward cation binding is one of the reasons for low stability of complexes **4b**•$EtNH_3^+$ and **5b**•$EtNH_3^+$ and dimers $(\mathbf{4a})_2$ and $(\mathbf{5a})_2$ in solutions.

The lengths of the N(1)H···O(2′,4′) and N(1′)H···O(1,3,4) hydrogen bonds are in the range of 1.94−2.20 Å, and the angles at hydrogen atoms are 126−179°. In one macrocycle, there is no hydrogen bond between the nitrogen atom and the ammonium ion (the shortest N(1′)H···N(3) distance is 3.23 Å). In the other macrocycle, there is the N(1)H···N(3′) hydrogen bond with parameters of 2.16 Å and 174°. The hydrogen bonding results in partial sp^3-hybridization of the N(3′) atom, which reduces conjugation of its lone electron pair with the chromophore electronic system, as indicated by the smaller sum of the bond angles at N(3′) compared with N(3) (346.8(3)° vs 358.3(4)°) and by longer N(3′)−C_{Ar} bond compared with the N(3)−C_{Ar} bond (1.405(5) vs 1.387(6) Å).

The styrylpyridinium unit of one of the independent dications in structure **4a** is disordered over two sites with an occupancy ratio of 0.83:0.17. This disorder is often observed in the crystals of stilbene-like compounds and is usually attributed to pedal, or crankshaft, motion of the ethylene unit,[35−37] which results in the dynamic coexistence of two single-bond conformers in the same site of the unit cell.

In the disordered dication, the geometry of the chromophore is nearly planar: the dihedral angles between the mean planes of the pyridine and benzene rings in the predominant and minor *s*-conformers are 3.5° and 3.6°, respectively. The chromophore moiety of the ordered dication is a little incurved (without twisting), the dihedral angle between the mean planes of the pyridine and benzene rings being 13.6°. The mean planes of the styrylpyridinium units of the two independent dications intersect at a large angle (61°). In this conformation of the dimeric complex, the stacking interactions between the chromophores should be very weak.

The distances between the carbon atoms of two ethylene bonds in the dimeric complex are in the range of 4.59−5.62 Å, and these bonds are nonparallel. According to topochemical criteria,[38,39] this virtually rules out the possibility of solid-phase PCA reaction.

3.1.4. Quantum-Chemical Modeling. The various conformations of pseudocyclic dimers $(\mathbf{1a})_2$ and $(\mathbf{3a})_2$ were first analyzed in the gas phase using the parametrized electronic structure model developed by Laikov[40] and implemented in the Priroda 14 program.[41] For the subsequent B3LYP-D3/PCM calculations, we selected 8 symmetrical structures differing in the conformation of the benzo(aza)-18-crown-6 ether moiety (*up* or *dn*, Chart 2), in the single-bond conformation of the chromophore (*s-trans* or *s-cis*), or in the relative orientation of the two chromophores (*syn*-head-to-tail or *anti*-head-to-tail). Full geometry optimizations were performed without symmetry constraints.

Chart 2. Conformer Notation

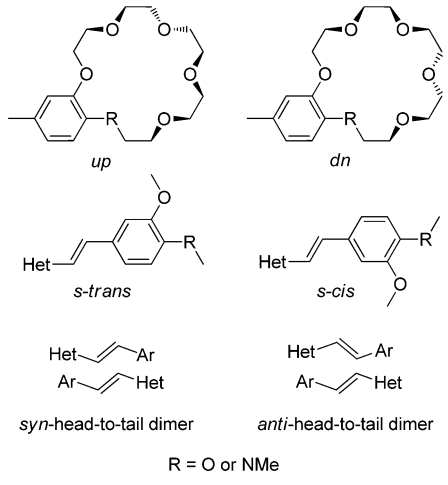

The most stable *syn*- and *anti*-conformers of dimer $(\mathbf{1a})_2$ are shown in Figure 4. The relative energies and fractional populations for all calculated conformers of $(\mathbf{1a})_2$ and $(\mathbf{3a})_2$ are summarized in Table 3, while the Cartesian coordinates are presented in the Supporting Information.

DOI: 10.1021/acs.jpca.5b10758
J. Phys. Chem. A XXXX, XXX, XXX−XXX

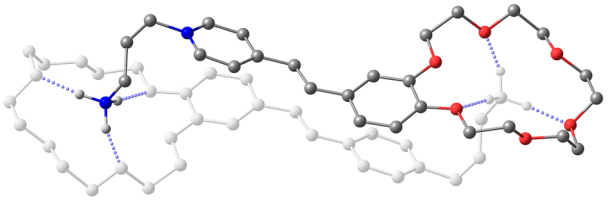

syn-(*s-cis-up*)$_2$

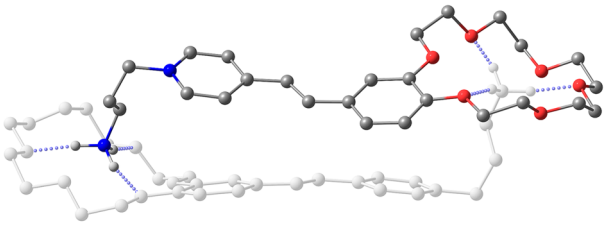

anti-(*s-cis-dn*)$_2$

Figure 4. Most stable *syn*- and *anti*-conformers of dimer (**1a**)$_2$ in MeCN, as calculated by the B3LYP-D3/PCM method.

Table 3. Theoretical Data for Different Symmetrical Conformers of Dimers (1a)$_2$ and (3a)$_2$ in MeCN[a]

	(**1a**)$_2$		(**3a**)$_2$	
conformer	E_{rel}	P	E_{rel}	P
anti-(*s-cis-dn*)$_2$	0	45.3	0.03	38.5
anti-(*s-cis-up*)$_2$	0.43	21.8	1.27	4.7
anti-(*s-trans-dn*)$_2$	0.72	13.3	0	40.8
syn-(*s-cis-up*)$_2$	1.35	4.6	1.67	2.4
syn-(*s-trans-up*)$_2$	1.39	4.2	1.62	2.6
anti-(*s-trans-up*)$_2$	1.40	4.1	1.34	4.1
syn-(*s-trans-dn*)$_2$	1.45	3.8	1.30	4.4
syn-(*s-cis-dn*)$_2$	1.61	2.9	1.63	2.5

[a]All structures are optimized by the B3LYP-D3/PCM method; E_{rel} is the relative energy in kcal mol^{-1}; P is the fractional population, %.

In the *syn*-conformers of (**1a**)$_2$ and (**3a**)$_2$, the olefinic bonds are parallel to each other, the distances between them varying over the ranges of 3.45−3.58 Å (**1a**) and 3.56−3.64 Å (**3a**). These geometries conform well to the criteria for PCA[38,39] and imply the formation of *syn*-head-to-tail cycloadducts, in agreement with the experimental data obtained for dye **1a**.[14,15] The dihedral angles between the pyridine and benzene rings of the chromophore are 15−22° for *syn*-(**1a**)$_2$ and 14−22° for *syn*-(**3a**)$_2$, the mean planes of the styrylpyridinium units being parallel to each other.

In the most stable *anti*-conformers, the dihedral angles between the pyridine and benzene rings of the chromophore are much smaller but the mean planes of the styrylpyridinium units intersect at a substantial angle. The C=C bonds in these structures adopt a criss-cross conformation unsuitable for PCA.

The total fractional population of *syn*-(**1a**)$_2$ is estimated to be 15.5%. Assuming that the quantum yield of PCA in *syn*-dimers corresponds to the theoretical maximum (i.e., two), one gets the overall quantum yield to be 0.31, which is smaller than 0.38 measured for (**1a**)$_2$ (see section 3.2). This means that either the calculations underestimate the population of *syn*-(**1a**)$_2$ or the molar absorption coefficients of the *syn*-conformers at the irradiation wavelength (436 nm) are higher than those of the *anti*-conformers due to substantial structural differences. The total fractional population of *syn*-(**3a**)$_2$ is predicted to be 11.9%.

The dimer of ammonioethyl dye **1b** was modeled in the symmetrical *syn*-(*s-cis*)$_2$ conformation observed in the crystal.[15] The geometrical characteristics of *syn*-(*s-cis*-**1b**)$_2$ calculated in solution (Figure 5) are very similar to those found in the

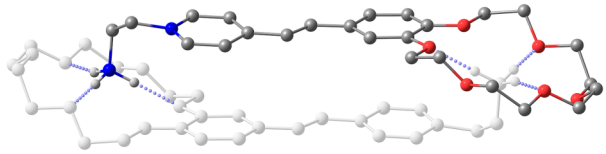

Figure 5. Geometry of *syn*-(*s-cis*-**1b**)$_2$ in MeCN, as calculated by the B3LYP-D3/PCM method.

crystal. The distance between the olefinic bonds is about 3.50 Å in the crystal and about 3.43 Å in solution. The dihedral angle between the pyridine and benzene rings of the chromophore is about 2° in the crystal and about 5° in solution, i.e., the chromophore geometry is nearly planar in both cases. This fact implies stronger stacking interactions between the chromophores in *syn*-(*s-cis*-**1b**)$_2$ compared to the *syn*-conformers of (**1a**)$_2$.

Among the numerous symmetrical conformations of dimer (**6a**)$_2$ calculated using the parametrized electronic structure model,[40] five most probable structures were selected and optimized by the B3LYP-D3/PCM method. Two most stable conformers are shown in Figure 6; they have nearly the same energy.

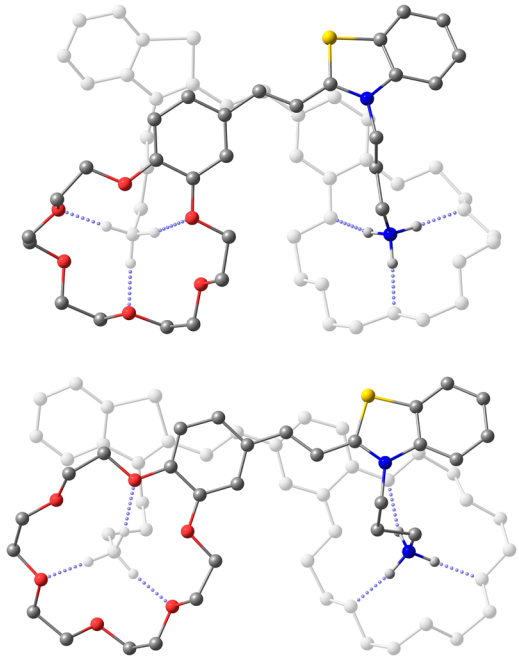

Figure 6. Most stable conformers of dimer (**6a**)$_2$ in MeCN, as calculated by the B3LYP-D3/PCM method.

The olefinic bonds in these conformers are not parallel to each other and are shifted relative to each other in the projection to the imaginary middle plane between the two chromophores. The Coulomb repulsion between the benzothiazolium cations may prevent these bonds from approaching each other. The distances between the ammonium ions are much shorter in the conformers of (**6a**)$_2$ (8.8 and 10.5 Å) than in the dimers of pyridinium dyes (14.5−15.4 Å). In addition,

DOI: 10.1021/acs.jpca.5b10758
J. Phys. Chem. A XXXX, XXX, XXX−XXX

the calculated structures imply the lack of stacking interactions between the aromatic and heteroaromatic residues.

3.1.5. Structure–Property Relationships. Analysis of the dimerization equilibrium constants for ammonium dyes and the stability constants for the 1:1 complexes of model compounds with $EtNH_3^+$ (Tables 1 and 2) reveals the following trends.

Macrocycle Size and Structure. The dimerization constant K_D varies depending on the crown ether moiety of the dye in the following order: benzo-15-crown-5 ≤ *N*-phenylaza-18-crown-6 ≤ *N*-methylbenzoaza-15-crown-5 ≪ benzo-18-crown-6 < *N*-methylbenzoaza-18-crown-6. The ability of these macrocycles to bind the primary ammonium ions varies in the same series. This correlation is due to the fact that the driving force for dimerization of dicationic dyes **1**–**6** is the macrocycle–ammonium ion interaction. The macrocyclic cavity size has a critical effect on the dimerization of benzo(aza)crown ether dyes. The macrocycle geometry of benzo-18-crown-6 ethers is close to optimal for the formation of three directional or six bifurcate hydrogen bonds with NH_3^+; therefore, they bind the primary ammonium ions much more efficiently than benzo-15-crown-5 ether analogues.[42,43]

In the case of azacrown ether dyes, the stability of pseudocyclic dimers is also critically affected by the type of coupling of the macrocycle with the benzene ring: the K_D constant for benzoazacrown ether **3a** is 5 orders of magnitude higher than that for related phenylazacrown ether **4a**. One reason for this huge difference in the K_D values is the fact that *N*-methylbenzoazacrown ethers are better preorganized toward cation binding than *N*-phenylazacrown ethers,[34] in particular, due to favorable orientation of the nitrogen lone pair.[44] Yet another and, probably, more significant reason is that the nitrogen atom in *N*-methylbenzoazacrown ethers is more basic[34] and, therefore, it forms a stronger hydrogen bond with NH_3^+. Owing to this feature, benzoazacrown ethers **3a,b** dimerize even more readily than analogous benzocrown ethers **1a,c**.

Nature of the Heteroaromatic Residue. The ability of the crown ether moiety of styryl dye to bind $EtNH_3^+$ depends weakly on the nature of the heteroaromatic core: the stability constants K_1 of the complexes formed by model dyes **1d**, **2c**, and **6b** containing pyridine, quinoline, and benzothiazole residues are very similar. Meanwhile, analogous dyes containing *N*-ammoniopropyl group (compounds **1a**, **2a**, and **6a**) differ significantly in the self-complexation behavior: the K_D value increases by more than an order of magnitude in the sequence **6a** < **1a** < **2a**. The key factor responsible for these differences is the stacking interactions between the chromophores in pseudocyclic dimers. It has been reported that stacking can have significant effects on both the structure and stability of dimeric complexes.[11−13] The important role of stacking interactions in the self-complexation of pyridine and quinoline derivatives is evidenced by the fact that the log K_D values for ammonium dyes **1a**–**5a** are more than twice greater than the log K_1 values for the corresponding model dyes.

The quinoline derivatives **2a** and **5a** form more stable dimers in comparison with the related pyridine derivatives **1a** and **4a**. The opposite situation is observed for the 1:1 complexes of model dyes with $EtNH_3^+$. This is due to the fact that more extended conjugated system in 4-styrylquinoline derivatives leads to stronger stacking interactions in the dimeric complex.

The results of B3LYP-D3/PCM calculations imply that much lower stability of dimers $(\mathbf{6a})_2$ compared to $(\mathbf{1a})_2$ and $(\mathbf{2a})_2$ is caused, first, by the lack of stacking interactions between the aromatic and heteroaromatic residues and, second, by stronger Coulomb repulsion between the NH_3^+ groups.

Spacer Length. Shorter spacers in dimer $(\mathbf{1b})_2$ compared to $(\mathbf{1a})_2$ ensure stronger stacking interactions between the pyridine and benzene rings (see B3LYP-D3/PCM calculations), which results in an increase in the dimerization equilibrium constant. The opposite effect observed for quinoline derivatives **2a,b** is, most likely, related to the steric interaction between the polymethylene chain and the quinoline ring. Because of steric hindrances, the less flexible ammonioethyl group in **2b** is unable to adopt the conformation that would ensure the most efficient self-complexation of the dye. This assumption is supported by comparing the conformations of dimers $(\mathbf{1b})_2$ and $(\mathbf{2b})_2$ in the crystal.[15] The steric influence of the annelated benzene ring on the dimerization of dye **2a** is less pronounced due to higher conformational flexibility of the ammoniopropyl group.

3.2. Supramolecular [2 + 2] Photocycloaddition. The stationary irradiation of dye **1a** in MeCN with 436 nm light leads to fast decoloration of the solution (Figure 7), due to the PCA reaction. The time dependence of the conversion to the cycloadduct in the initial stage of photolysis (inset in Figure 7) is described by the kinetic equation for irreversible unimolecular photoreactions eq 3. This is due to the following factors: first, at ~10^{-5} M concentrations, dye **1a** is almost completely dimerized (log K_D = 7.3), second, the cycloadduct does not absorb light with λ = 436 nm; and third, the quantum yield of *E*–*Z* photoisomerization in dimers $(\mathbf{1a})_2$ is negligibly low as compared with the PCA quantum yield. Qualitatively similar photochemical properties are exhibited by dyes **1b** and **2a,b** (Figures S32–S34 in the Supporting Information).

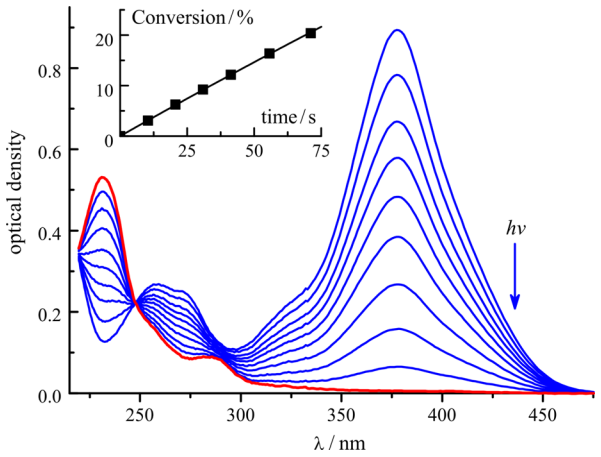

Figure 7. Steady-state photolysis of dye **1a** in MeCN with 436 nm light; 1 cm cell, $C_L = 2.9 \times 10^{-5}$ M, ionic strength 0.01 M, light intensity 8.7×10^{-6} einstein m^{-2} c^{-1}, irradiation time (min): 0, 0.7, 1.5, 2.3, 3.2, 4.4, 6.2, 9.0, 14.0, and 60 (red curve). Inset: percentage of conversion of **1a** as a function of the irradiation time; the solid curve is from global fitting to eq 3.

Table 4 presents the quantum yields of the PCA reaction in the supramolecular dimers of ammonium dyes **1**–**6** in MeCN. The dimers of styrylpyridine and styrylquinoline derivatives having ammoniopropyl spacers, $(\mathbf{1a})_2$, $(\mathbf{1c})_2$, and $(\mathbf{2a})_2$, undergo this photoreaction very readily owing to favorable relative positions and rather high mobility of the olefinic bonds in the *syn*-conformers (see section 3.1.4). Comparison of the $\varphi_{[2+2]}$ values measured for $(\mathbf{1a})_2$ and $(\mathbf{1c})_2$ suggests that the

DOI: 10.1021/acs.jpca.5b10758
J. Phys. Chem. A XXXX, XXX, XXX–XXX

Table 4. Quantum Yields of the [2 + 2] Photocycloaddition Reaction in the Supramolecular Dimers of Ammonium Dyes 1−6, $\varphi_{[2+2]}$, and Key Spectrophotometric Characteristics of Cycloadducts[a]

		data for cycloadducts	
dimer	$\varphi_{[2+2]}$	λ_{max}	$\varepsilon \times 10^{-4}$
$(\mathbf{1a})_2$	0.38	286	0.62
$(\mathbf{1b})_2$	0.049	288	0.64
$(\mathbf{1c})_2$	0.26	286	0.58
$(\mathbf{2a})_2$	0.27	319	1.38
$(\mathbf{2b})_2$	0.0065	321	1.14
$(\mathbf{3a})_2$	$\leq 10^{-4}$		
$(\mathbf{3b})_2$	$\leq 10^{-4}$		
$(\mathbf{4a})_2$	$\leq 10^{-4}$		
$(\mathbf{5a})_2$	$\leq 10^{-4}$		
$(\mathbf{6a})_2$	$<10^{-4}$		

[a]In MeCN; λ_{max} is the long-wavelength absorption maximum, nm; ε is the molar absorption coefficient at λ_{max}, M^{-1} cm^{-1}.

macrocycle size in the dye affects only slightly the relative positions of the chromophores in the dimer.

Analogues of dimers $(\mathbf{1a})_2$ and $(\mathbf{2a})_2$ having shorter (ammonioethyl) spacers, $(\mathbf{1b})_2$ and $(\mathbf{2b})_2$, show much lower PCA quantum yields: in the case of pyridine derivatives, the $\varphi_{[2+2]}$ value drops 8-fold, while in the case of quinoline derivatives, it drops 40-fold. Note that distances between the parallel olefinic bonds in dimers $(\mathbf{1b})_2$ and $(\mathbf{2b})_2$ in the crystalline state are virtually equal (3.50 vs 3.49 Å).[15] Furthermore, according to B3LYP-D3/PCM calculations, the arrangement of the olefinic bonds in *syn*-$(\mathbf{1b})_2$ in solution is not less favorable for PCA than in *syn*-$(\mathbf{1a})_2$.

The most likely reason for lower photoreactivity of $(\mathbf{1b})_2$ compared to $(\mathbf{1a})_2$ is lower conformational flexibility of the ammonioethyl spacers restricting the mobility of olefinic bonds. In dimer $(\mathbf{2b})_2$, the steric interaction of the annelated benzene ring of quinoline with the dimethylene chain is one more factor reducing the conformational flexibility of the pseudocycle; therefore, the effect of the spacer length on the dimer photoreactivity is most pronounced for quinoline derivatives.

Note that model dye **1d** undergoes *E*−*Z* photoisomerization in MeCN with a quantum yield of 0.17, which increases upon complexation of **1d** with ammonium ions.[45] Photochemical studies of the dimer−monomer equilibrium mixtures with high monomer contents (in MeCN−H_2O solutions) revealed that the monomers of dyes **1a−c** also undergo this photoreaction, unlike the dimers. The inefficiency of geometric photoisomerization in the pseudocyclic dimers of **1a−c** is apparently due to significant steric hindrance for rotation around the C=C double bond. Yet another possible reason is rapid conversion of the locally excited state to a delocalized excimer state, followed by deactivation along two pathways:[46] [2 + 2] cycloaddition (*syn*-conformers) and internal conversion to the ground state (*syn*- and *anti*-conformers).

The monomers of azacrown ether dyes **3−5** virtually do not undergo *E*−*Z* photoisomerization in polar solvents due to rapid conversion of the initial excited state to the twisted internal charge-transfer (TICT) state,[34,47] which is deactivated without geometric isomerization. This feature is associated with strong electron-donating ability of benzoazacrown and phenylazacrown ether moieties.

The irradiation of pseudocyclic dimers of azacrown-containing dyes **3a,b**, **4a**, and **5a** in MeCN with 436 nm light for several hours induced only minor changes in the absorption spectra. The inefficiency of PCA in $(\mathbf{4a})_2$ and $(\mathbf{5a})_2$ is attributable to unfavorable geometric factors related to specific conformational properties of the *N*-phenylaza-18-crown-6-crown ether moiety (see the crystal structure of dimer $(\mathbf{4a})_2$ in Figure 3). It is more difficult to interpret the photochemical inertness of dimers $(\mathbf{3a})_2$ and $(\mathbf{3b})_2$ containing benzoazacrown ether moieties. According to B3LYP-D3/PCM calculations, the *syn*-conformers of $(\mathbf{3a})_2$ differ little in the geometric characteristics from the corresponding conformers of dimer $(\mathbf{1a})_2$, which readily undergoes PCA. The distances between the parallel olefinic bonds in the *syn*-conformers of $(\mathbf{3a})_2$ are longer than in $(\mathbf{1a})_2$ but the difference is only 0.06−0.11 Å, which can hardly be responsible for the contrasting difference in photoreactivity between these dimers. The fractional populations of *syn*-conformers of $(\mathbf{1a})_2$ and $(\mathbf{3a})_2$ are comparable in magnitude.

Presumably, the inefficiency of PCA in dimers $(\mathbf{3a})_2$ and $(\mathbf{3b})_2$ is related to fast photoinduced recoordination reaction typical of complexes of azacrown-containing styryl dyes with monocations.[34] The recoordination implies disruption of the hydrogen bond between the ammonium ion and the macrocycle nitrogen atom immediately after electronic excitation of the chromophore. This can be followed by nonradiative deactivation via the TICT state or via charge transfer between the two chromophores (note that dimers $(\mathbf{3a})_2$ and $(\mathbf{3b})_2$ virtually do not luminesce).

The pseudocyclic dimers of benzothiazole derivative **6a** do not undergo PCA but, in contrast to dimers of pyridine and quinoline derivatives, they can undergo *E*−*Z* photoisomerization. According to B3LYP-D3/PCM calculations, the relative positions of the olefinic bonds in the most probable conformers of $(\mathbf{6a})_2$ are unfavorable for PCA (see Figure 6); in addition, the Coulomb repulsion between the benzothiazolium cations can prevent these bonds from approaching to each other. In the case of $(\mathbf{6a})_2$, photoinduced rotation around the C=C double bond is sterically less hindered due to the specific pseudocycle geometry, the excimer formation being unlikely because of the lack of stacking interactions between the aromatic and heteroaromatic residues.

4. CONCLUSIONS

This study identified the key factors determining the thermodynamic stability and photochemical reactivity of the pseudocyclic dimers spontaneously formed by styryl dyes containing a crown ether moiety and a remote ammonium group.

The driving force of the supramolecular dimerization is the double macrocycle−ammonium ion interaction; therefore, the thermodynamic stability of dimers is critically affected by the size and structure of the macrocyclic moiety in the dye. The *N*-methylbenzoaza-18-crown-6 ether moiety provides the highest stability of pseudocyclic dimers. A noticeable role in the self-complexation of the dyes is played by stacking interactions. The strength of these interactions in the dimer depends on the nature of the heteroaromatic residue in the dye, the length of the ammonioalkyl group attached to this residue and the position of this group relative to the crown ether moiety. The latter factor is very important, as it dictates the relative position of styryl moieties in the dimer (*cf.* data obtained for related pyridine and benzothiazole derivatives). A decrease in the ammonioalkyl spacer length may increase the stability of the pseudocyclic dimer owing to enhancement of the stacking interactions but can also induce the opposite effect if there are

DOI: 10.1021/acs.jpca.5b10758
J. Phys. Chem. A XXXX, XXX, XXX−XXX

substantial steric interactions between the polymethylene chain and substituents in the heteroaromatic residue.

The [2 + 2] photocycloaddition in the pseudocyclic dimers is actually unimolecular, and therefore, there is no correlation between the dimerization equilibrium constant K_D and the reaction quantum yield $\varphi_{[2+2]}$. The relative position of the two olefinic bonds in the dimer is not the only factor having a critical effect on $\varphi_{[2+2]}$. Two other factors that can dramatically affect the supramolecular photocycloaddition are the electronic structure of styryl moieties, as dependent on the electron-donating ability of the substituents on the benzene ring, and the conformational flexibility of the pseudocycle, which determines the mobility of the olefinic bonds. A clear demonstration of the significance of the electronic factor is the contrasting difference between the photoreactivities of dimers $(\mathbf{1a})_2$ and $(\mathbf{3a})_2$ having very similar geometrical characteristics. The inefficiency of supramolecular photocycloaddition of dyes **3a,b** is associated with high electron-donating ability of *N*-methylbenzoazacrown ether moieties. Detailed interpretation of the photochemical inertness of $(\mathbf{3a})_2$ and $(\mathbf{3b})_2$ is a challenge, which may require additional experimental and theoretical efforts.

The results of this study can be used in the development of supramolecular approaches to control [2 + 2] photocycloaddition, *E*−*Z* photoisomerization, and other photochemical reactions and for rational design of supramolecular systems functioning as photoswitches, optical sensors, and so on.

■ ASSOCIATED CONTENT

Supporting Information

The Supporting Information is available free of charge on the ACS Publications website at DOI: 10.1021/acs.jpca.5b10758.

^{1}H and ^{13}C NMR spectra of synthesized compounds, spectrophotometric and ^{1}H NMR spectroscopic data on supramolecular dimerization of styryl dyes, data on photolysis of dimeric complexes, B3LYP-D3/PCM calculated energies and Cartesian coordinates of dimeric complexes, and electrochemical data for selected styryl dyes and cyclobutanes (PDF)

■ AUTHOR INFORMATION

Corresponding Authors

*(E.N.U.) Telephone: +7 496 5245446. Fax: +7 496 5223507. E-mail: e.n.ushakov@gmail.com.

*(S.P.G.) Telephone: +7 495 9350116. Fax: +7 495 9361255. E-mail: spgromov@mail.ru.

Notes

The authors declare no competing financial interest.

■ ACKNOWLEDGMENTS

This work was supported by the Russian Science Foundation (Project No. 14-13-00076) and by the Russian Foundation for Basic Research (studies on the self-complexation of *N*-methylbenzoazacrown ether compounds). The X-ray diffraction study of dye **4a** was performed under support of the Russian Academy of Sciences. L.G.K. thanks the Royal Society of Chemistry for International Author Grant.

■ REFERENCES

(1) Hoffmann, N. Photochemical Reactions as Key Steps in Organic Synthesis. *Chem. Rev.* **2008**, *108*, 1052−1103.

(2) Bach, T.; Hehn, J. P. Photochemical Reactions as Key Steps in Natural Product Synthesis. *Angew. Chem., Int. Ed.* **2011**, *50*, 1000−1045.

(3) Sonoda, Y. Solid-State [2 + 2] Photodimerization and Photopolymerization of *α,ω*-Diarylpolyene Monomers: Effective Utilization of Noncovalent Intermolecular Interactions in Crystals. *Molecules* **2011**, *16*, 119−148.

(4) Alfimov, M. V.; Gromov, S. P.; Stanislavskii, O. B.; Ushakov, E. N.; Fedorova, O. A. Crown-Containing Styryl Dyes. 8. Cation-Dependent Concerted [2 + 2] Autophotocycloaddition of Photochromic 15-Crown-5 Ether Betaines. *Russ. Chem. Bull.* **1993**, *42*, 1385−1389.

(5) Hirayama, F.; Utsuki, T.; Uekama, K. Stoichiometry-Dependent Photodimerization of Tranilast in a *γ*-Cyclodextrin Inclusion Complex. *J. Chem. Soc., Chem. Commun.* **1991**, 887−888.

(6) Bibal, B.; Mongin, C.; Bassani, D. M. Template Effects and Supramolecular Control of Photoreactions in Solution. *Chem. Soc. Rev.* **2014**, *43*, 4179−4198.

(7) Ushakov, E. N.; Gromov, S. P. Supramolecular Methods for Controlling Intermolecular [2 + 2] Photocycloaddition Reactions of Unsaturated Compounds in Solutions. *Russ. Chem. Rev.* **2015**, *84*, 787−802.

(8) Ramamurthy, V.; Mondal, B. Supramolecular Photochemistry Concepts Highlighted with Select Examples. *J. Photochem. Photobiol., C* **2015**, *23*, 68−102.

(9) Shinkai, S.; Yoshida, T.; Miyazaki, K.; Manabe, O. Photoresponsive Crown Ethers. 19. Photocontrol of Reversible Association-Dissociation Phenomena in "Tail(Ammonium)-Biting" Crown Ethers. *Bull. Chem. Soc. Jpn.* **1987**, *60*, 1819−1824.

(10) Cantrill, S. J.; Youn, G. J.; Stoddart, J. F.; Williams, D. J. Supramolecular Daisy Chains. *J. Org. Chem.* **2001**, *66*, 6857−6872.

(11) Kryatova, O. P.; Kryatov, S. V.; Staples, R. J.; Rybak-Akimova, E. V. Stable Supramolecular Dimer of Self-Complementary Benzo-18-Crown-6 with a Pendant Protonated Amino Arm. *Chem. Commun.* **2002**, 3014−3015.

(12) Zheng, B.; Zhang, M.; Dong, S.; Liu, J.; Huang, F. A Benzo-21-Crown-7/Secondary Ammonium Salt [*c*2]Daisy Chain. *Org. Lett.* **2012**, *14*, 306−309.

(13) Amirsakis, D. G.; Elizarov, A. M.; Garcia-Garibay, M. A.; Glink, P. T.; Stoddart, J. F.; White, A. J. P.; Williams, D. J. Diastereospecific Photochemical Dimerization of a Stilbene-Containing Daisy Chain Monomer in Solution as well as in the Solid State. *Angew. Chem., Int. Ed.* **2003**, *42*, 1126−1132.

(14) Gromov, S. P.; Lobova, N. A.; Vedernikov, A. I.; Kuz'mina, L. G.; Howard, J. A. K.; Alfimov, M. V. Stereospecific [2 + 2] Autophotocycloaddition in the Dimeric Complex of 18-Crown-6 Ether Styryl Dye Bearing *N*-(3-Ammoniopropyl) Substituent. *Russ. Chem. Bull.* **2009**, *58*, 1211−1216.

(15) Gromov, S. P.; Vedernikov, A. I.; Lobova, N. A.; Kuz'mina, L. G.; Dmitrieva, S. N.; Strelenko, Yu. A.; Howard, J. A. K. Synthesis, Structure, and Properties of Supramolecular Photoswitches Based on Ammonioalkyl Derivatives of Crown Ether Styryl Dyes. *J. Org. Chem.* **2014**, *79*, 11416−11430.

(16) Atabekyan, L. S.; Vedernikov, A. I.; Avakyan, V. G.; Lobova, N. A.; Gromov, S. P.; Chibisov, A. K. Photoprocesses in Styryl Dyes and Their Pseudorotaxane Complexes with Cucurbit[7]uril. *J. Photochem. Photobiol., A* **2013**, *253*, 52−61.

(17) Vedernikov, A. I.; Kondratuk, D. V.; Lobova, N. A.; Valova, T. M.; Barachevskii, V. A.; Alfimov, M. V.; Gromov, S. P. New Cation-"Capped" Complex of the *Z*-Isomer of a Crown-Containing Styryl Dye Bearing a Long *N*-Ammonioalkyl Substituent. *Mendeleev Commun.* **2007**, *17*, 264−267.

(18) Fedorova, O. A.; Andryukhina, E. N.; Lindeman, A. V.; Basok, S. S.; Bogaschenko, T. Yu.; Gromov, S. P. Synthesis of Crown-Containing 2-Styrylbenzothiazoles. Effect of Alkali Metal Cations on the Condensation of Crown-Ether Benzaldehydes with 2-Methylbenzothiazole. *Russ. Chem. Bull.* **2002**, *51*, 319−325.

DOI: 10.1021/acs.jpca.5b10758
J. Phys. Chem. A XXXX, XXX, XXX−XXX

(19) Koral, M.; Bonis, D.; Fusco, A. J.; Dougherty, P.; Leifer, A.; LuValle, J. E. The Synthesis of Some Heterocyclic Quaternary Amine Iodides. *J. Chem. Eng. Data* **1964**, *9*, 406−407.
(20) Gribaudo, M. L.; Knorr, F. J.; McHale, J. L. Equilibrium Constants and Optical Spectra of 1:1 and 2:1 Electron Donor−Acceptor Complexes with Overlapping Bands. *Spectrochim. Acta, Part A* **1985**, *41*, 419−424.
(21) Ushakov, E. N.; Gromov, S. P.; Fedorova, O. A.; Pershina, Yu. V.; Alfimov, M. V.; Barigelletti, F.; Flamigni, L.; Balzani, V. Sandwich-Type Complexes of Alkaline-Earth Metal Cations with a Bisstyryl Dye Containing Two Crown Ether Units. *J. Phys. Chem. A* **1999**, *103*, 11188−11193.
(22) Frassineti, C.; Ghelli, S.; Gans, P.; Sabatini, A.; Moruzzi, M. S.; Vacca, A. Nuclear Magnetic Resonance as a Tool for Determining Protonation Constants of Natural Polyprotic Bases in Solution. *Anal. Biochem.* **1995**, *231*, 374−382.
(23) *SHELXTL-Plus*, Version 5.10; Bruker AXS, Inc.: Madison, WI, 1997.
(24) Dolomanov, O. V.; Bourhis, L. J.; Gildea, R. J.; Howard, J. A. K.; Puschmann, H. OLEX2: a Complete Structure Solution, Refinement and Analysis Program. *J. Appl. Crystallogr.* **2009**, *42*, 339−341.
(25) *Gaussian 09*, Revision D.01; Gaussian, Inc.: Wallingford, CT, 2013.
(26) Becke, A. D. Density-Functional Thermochemistry. III. The Role of Exact Exchange. *J. Chem. Phys.* **1993**, *98*, 5648−5652.
(27) Grimme, S.; Ehrlich, S.; Goerigk, L. Effect of the Damping Function in Dispersion Corrected Density Functional Theory. *J. Comput. Chem.* **2011**, *32*, 1456−1465.
(28) Cossi, M.; Rega, N.; Scalmani, G.; Barone, V. Energies, Structures, and Electronic Properties of Molecules in Solution with the C-PCM Solvation Model. *J. Comput. Chem.* **2003**, *24*, 669−681.
(29) Löhr, H.-G.; Vögtle, F. Chromo- and Fluoroionophores. A New Class of Dye Reagents. *Acc. Chem. Res.* **1985**, *18*, 65−72.
(30) Ushakov, E. N.; Alfimov, M. V.; Gromov, S. P. Design Principles for Optical Molecular Sensors and Photocontrolled Receptors Based on Crown Ethers. *Russ. Chem. Rev.* **2008**, *77*, 39−58.
(31) Yuzhakov, V. I. Association of Dye Molecules and Its Spectroscopic Manifestation. *Russ. Chem. Rev.* **1979**, *48*, 1076−1091.
(32) Ushakov, E. N.; Vedernikov, A. I.; Alfimov, M. V.; Gromov, S. P. Regio- and Stereospecific [2 + 2] Photocyclodimerization of a Crown-Containing Butadienyl Dye via Cation-Induced Self-Assembly in Solution. *Photochem. Photobiol. Sci.* **2011**, *10*, 15−18.
(33) Solov'ev, V. P.; Strakhova, N. N.; Raevsky, O. A.; Rüdiger, V.; Schneider, H.-J. Solvent Effects on Crown Ether Complexations. *J. Org. Chem.* **1996**, *61*, 5221−5226.
(34) Gromov, S. P.; Dmitrieva, S. N.; Vedernikov, A. I.; Kurchavov, N. A.; Kuz'mina, L. G.; Sazonov, S. K.; Strelenko, Yu. A.; Alfimov, M. V.; Howard, J. A. K.; Ushakov, E. N. Synthesis, Structure, and Characterization of Chromo(fluoro)ionophores with Cation-Triggered Emission Based on *N*-Methylaza-Crown-Ether Styryl Dyes. *J. Org. Chem.* **2013**, *78*, 9834−9847.
(35) Harada, J.; Ogawa, K. X-ray Diffraction Analysis of Non-equilibrium States in Crystals: Observation of an Unstable Conformer in Flash-Cooled Crystals. *J. Am. Chem. Soc.* **2004**, *126*, 3539−3544.
(36) Harada, J.; Ogawa, K. Pedal Motion in Crystals. *Chem. Soc. Rev.* **2009**, *38*, 2244−2252.
(37) Elacqua, E.; Kaushik, P.; Groeneman, R. H.; Sumrak, J. C.; Bučar, D.-K.; MacGillivray, L. R. A Supramolecular Protecting Group Strategy Introduced to the Organic Solid State: Enhanced Reactivity through Molecular Pedal Motion. *Angew. Chem., Int. Ed.* **2012**, *51*, 1037−1041.
(38) Schmidt, G. M. J. Photodimerization in the Solid State. *Pure Appl. Chem.* **1971**, *27*, 647−678.
(39) Ramamurthy, V.; Venkatesan, K. Photochemical Reactions of Organic Crystals. *Chem. Rev.* **1987**, *87*, 433−481.
(40) Laikov, D. N. A New Parametrizable Model of Molecular Electronic Structure. *J. Chem. Phys.* **2011**, *135*, 134120.
(41) Laikov, D. N. *Priroda 14. Quantum Chemical Program*, Version 2014.02.23; Lomonosov Moscow State University: Moscow, 2014.
(42) Izatt, R. M.; Pawlak, K.; Bradshaw, J. S.; Bruening, R. L. Thermodynamic and Kinetic Data for Macrocycle Interaction with Cations and Anions. *Chem. Rev.* **1991**, *91*, 1721−2085.
(43) Späth, A.; König, B. Molecular Recognition of Organic Ammonium Ions in Solution Using Synthetic Receptors. *Beilstein J. Org. Chem.* **2010**, *6* (32), 111.
(44) Solov'ev, V. P.; Strakhova, N. N.; Kazachenko, V. P.; Solotnov, A. F.; Baulin, V. E.; Raevsky, O. A.; Rüdiger, V.; Eblinger, F.; Schneider, H.-J. Steric and Stereoelectronic Effects in Aza Crown Ether Complexes. *Eur. J. Org. Chem.* **1998**, *1998*, 1379−1389.
(45) Ushakov, E. N.; Vedernikov, A. I.; Sazonov, S. K.; Kuz'mina, L. G.; Alfimov, M. V.; Howard, J. A. K.; Gromov, S. P. Synthesis and Photochemical Study of a Supramolecular Pseudodimeric Complex of 4-Styrylpyridinium Derivatives. *Russ. Chem. Bull.* **2015**, *64*, 562−572.
(46) Yuan, S.; Hong, H.; Wang, G.; Zhang, W.; Dou, Y.; Lo, G. V. Competing Deactivation Channels for Excited π-Stacked Cytosines. *Int. J. Photoenergy* **2014**, *2014*, 1−9.
(47) Grabowski, Z. R.; Rotkiewicz, K.; Rettig, W. Structural Changes Accompanying Intramolecular Electron Transfer: Focus on Twisted Intramolecular Charge-Transfer States and Structures. *Chem. Rev.* **2003**, *103*, 3899−4031.

DOI: 10.1021/acs.jpca.5b10758
J. Phys. Chem. A XXXX, XXX, XXX−XXX